Nuclear Engineering and Technology 54 (2022) 3073–3084

Contents lists available at ScienceDirect

Nuclear Engineering and Technology

journal homepage: www.elsevier.com/locate/net

Original Article

Propagation of radiation source uncertainties in spent fuel cask shielding calculations

Bamidele Ebiwonjumi [a], Nhan Nguyen Trong Mai [a], Hyun Chul Lee [b], Deokjung Lee [a, *]

[a] Department of Nuclear Engineering, Ul san National Institute of Science and Technology, 50 UNIST-gil, Ulsan, 44919, Republic of Korea
[b] Nuclear Engineering Division, School of Mechanical Engineering, Pusan National University, 2, Busandaehak-ro, 63 Beon-gil, Geumjeong-gu, Busan, 46241, Republic of Korea

ARTICLE INFO

Article history:
Received 1 December 2021
Received in revised form
11 February 2022
Accepted 2 March 2022
Available online 3 March 2022

Keywords:
Monte Carlo shielding
STREAM
Spent nuclear fuel
Uncertainty quantification
Stochastic sampling

ABSTRACT

The propagation of radiation source uncertainties in spent nuclear fuel (SNF) cask shielding calculations is presented in this paper. The uncertainty propagation employs the depletion and source term outputs of the deterministic code STREAM as input to the transport simulation of the Monte Carlo (MC) codes MCS and MCNP6. The uncertainties of dose rate coming from two sources: nuclear data and modeling parameters, are quantified. The nuclear data uncertainties are obtained from the stochastic sampling of the cross-section covariance and perturbed fission product yields. Uncertainties induced by perturbed modeling parameters consider the design parameters and operating conditions. Uncertainties coming from the two sources result in perturbed depleted nuclide inventories and radiation source terms which are then propagated to the dose rate on the cask surface. The uncertainty analysis results show that the neutron and secondary photon dose have uncertainties which are dominated by the cross section and modeling parameters, while the fission yields have relatively insignificant effect. Besides, the primary photon dose is mostly influenced by the fission yield and modeling parameters, while the cross-section data have a relatively negligible effect. Moreover, the neutron, secondary photon, and primary photon dose can have uncertainties up to about 13%, 14%, and 6%, respectively.

1. Introduction

This work is a continuation of our previous studies on radiation source terms of pressurized water reactor (PWR) spent nuclear fuel (SNF). The deterministic reactor analysis code STREAM is developed for light water reactor (LWR) whole core analysis [1] and to support SNF applications in deep penetration problems, radiation shielding and cask analysis [2]. STREAM depletion and radiation source term calculation capabilities are validated using measured PWR SNF isotopic compositions [3] and fuel assembly (FA) decay heat [4]. Moreover, the uncertainty quantification (UQ) of radiation source terms was recently conducted [5]. STREAM is used to generate depleted isotopic inventory and neutron/gamma radiation sources for SNF assembly cask eigenvalue and dose rate calculations. However, the effect of uncertainties present in the isotopic inventory and source terms on the cask shielding calculations are yet to be investigated. Several studies have propagated the bias and uncertainties of SNF nuclide inventory to eigenvalue calculations of spent fuel storage systems from the point of view of criticality safety and burnup credit [6–8]. As a result, these studies are mostly focused on the effective multiplication factor of the SNF in storage systems. However, the propagation of neutron and photon source uncertainties in cask radiation dose rate calculation is often neglected. Such investigation has not been considered by any study in literature and is important from the point of view of radiation shielding applications. The focus of this paper is to address this gap. This UQ study is important to give an order of magnitude to the dose rate uncertainties in the form of confidence intervals or lower and upper bounds, in ensuing that safety criteria are met. Although uncertainties in the effective multiplication factor of SNF cask are reported in this study, the burnup credit criticality safety analysis of such storage systems are not discussed in detail because they are not the focus of this work. Moreover, the uncertainties resulting from the bias of isotopic concentrations when compared to measured data [9], thus, are not considered in this work.

Uncertainty analysis of calculation results is important after the

* Corresponding author.
E-mail addresses: bamidele.ebiwonjumi@gmail.com (B. Ebiwonjumi), mainhan@unist.ac.kr (N.N. Trong Mai), hyunchul.lee@pusan.ac.kr (H.C. Lee), deokjung@unist.ac.kr (D. Lee).

https://doi.org/10.1016/j.net.2022.03.001

validation of codes developed for safety and licensing applications. This is usually realized by perturbing the code input data which have uncertainty information and then applying the perturbed inputs in many repeated calculations. The uncertainties in the code results are obtained by statistically post-processing the perturbed outputs. This approach, which is often referred to as forward UQ, and uses input data that are perturbed by stochastic sampling (SS), is the approach employed in this paper. In many nuclear engineering reactor physics codes, the input data are nuclear data (*e.g.*, nuclear reaction cross section, decay data, fission yields) and modelling parameters such as material, geometry, design parameters and operating conditions. UQ in cask criticality analysis is most often realized by a many-step approach. This entails (*i*) perturbation and sampling of nuclear data covariances using codes such as TSUNAMI [10] and SAMPLER [11] (*ii*) generation of problem dependent cross-section from each perturbed nuclear data library (*iii*) generation of depleted nuclide concentration using codes such as ORIGEN [12] (*iv*) criticality analysis with Monte Carlo (MC) particle transport codes such as KENO [13], MCNP6 [14] and MCS [15]. Studies on cask dose rate analysis can use the two-step approach *i.e.*, deterministic codes such as TORT or DENOVO, are used to calculate the adjoint solution of the problem. The adjoint or importance function as it is called, is then used to generate variance reduction parameters to speed up the MC simulation of codes such as MCNP [16,17], and MONACO [18]. The codes used to calculate the dose rates in an SNF cask are mostly MC codes. As a result, only the statistical uncertainties arising from the MC simulations are reported in literature [19,20].

In this study, the effect of radiation source term uncertainties on cask dose rate calculations is investigated. We propagate the uncertainties coming from cross-section, fission product yields, manufacturing tolerances and operating conditions. These uncertainties are first propagated to the depleted nuclide concentrations, neutron and photon sources at the end of life. This step is performed using the STREAM code which combines the stochastic sampling of cross section covariance, and generation of problem dependent cross section with depletion calculations. In the second step, the uncertainties of nuclide concentrations and the radiation sources are propagated to the cask eigenvalue and dose rates using the MC codes MCS and MCNP6. The two steps are summarized in Fig. 1 and are made possible by python scripts developed for two purposes: (*i*) extract depleted nuclide concentrations and source spectra from STREAM output files (*ii*) write the extracted outputs into input files for the MC codes. The TN-32 spent fuel dry storage cask and a PWR Westinghouse 15 × 15 fuel assembly are used to perform the uncertainty analysis. The goal of this study is to evaluate the uncertainties present in the dose rates estimated on the surface of this cask. The remainder of this paper is organized as follows. The TN-32 cask is presented in Section 2. This section also contain the modeling parameters and uncertainty information of the fuel assembly loaded into the cask. Section 3 describes the MCS and STREAM codes. Section 4 discusses the assembly neutron and gamma source spectra, their uncertainties, and the results of dose rate uncertainties due to nuclear data and modeling parameters uncertainties. The conclusions are outlined in Section 5.

2. Description of TN-32 spent nuclear fuel cask

The TN-32 cask is designed for dry storage conditions to load 32 spent fuel assemblies [21]. To ensure subcriticality of the arrangement, boron absorbers are placed between the assemblies and the cask has an inner waterproof design. The cask has a 5.2 m height and 2.5 m outer diameter. To provide radial shielding, the body of the cask is a 24.13 cm thick steel wall surrounded by a neutron shielding of 12.725 cm thick layer. Axial shielding is ensured by the top and bottom steel and neutron absorber. The radial and axial schematic of the cask is depicted in Fig. 2. The TN-32 cask satisfies 10 CFR 72 regulatory requirements [22] for spent fuel storage and can be used to store high burnup Westinghouse type fuel assemblies [23].

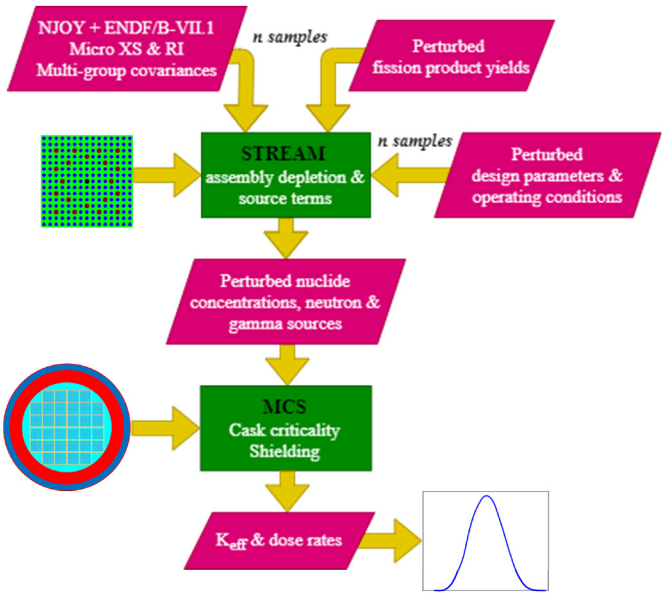

Fig. 1. Propagation of uncertainties from nuclear data and modeling parameters to spent fuel cask characteristics. Each group of data is perturbed *n* times. The STREAM/MCS calculations are performed 3*n* times.

A Westinghouse 15 × 15 fuel assembly design is selected to be loaded into the TN-32 cask. This assembly was discharged from Ringhals-2 PWR operated in Sweden. This assembly has decay heat measurement [24] which was used for validation and uncertainty analysis in our previous studies. The assembly, designated as C01, has 3.1 wt% ^{235}U enrichment, 36.7 GWd/tU discharge burnup, and 365.8 cm height of active fuel. The assembly consists of 204 UO_2 fuel rods, without burnable poison of absorber rods, one instrument tube, and 20 guide tubes. The radial layout of the assembly is illustrated in Fig. 3. The assembly was irradiated in four cycles with a cooling time of 23 years after discharge before the decay heat was measured.

Listed in Table 1 are the assembly design parameters and operating condition perturbations which are considered as uncertainty in this study. Other modeling parameters of the assembly which are not considered as uncertain are presented in Table 2. The modeling parameters uncertainties in Table 1 are referenced from literature [25,26]. We assumed that these parameters follow a uniform distribution. We applied the same uncertainty information to all the fuel pins, for each input parameter. The power density used in burnup calculation is perturbed at the beginning of each of the four cycles. The benchmark document gives cycle-averaged power history information for the assembly. The fuel/moderator temperature and boron concentration are only perturbed at the beginning of the first cycle. Then the subsequent cycles use the same perturbed values. This is because the benchmark documentation does not contain the fuel/moderator temperature and boron concentration histories, only average values over the entire burnup are reported. Although, as the burnup progresses, uncertainties in the modeling parameters might be affected, the burnup induced changes in the modeling parameters caused by the burnup are not accounted for. Examples of such changes are densification effects, irradiation swelling, pellet-clad gap thermomechanical interactions, bowing and rod deformation.

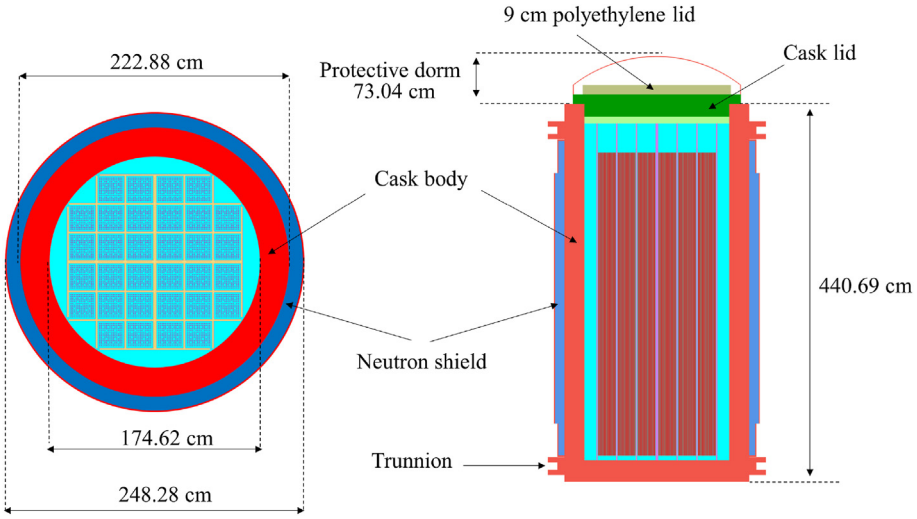

Fig. 2. Radial and axial layout of TN-32 cask generated by MCS code.

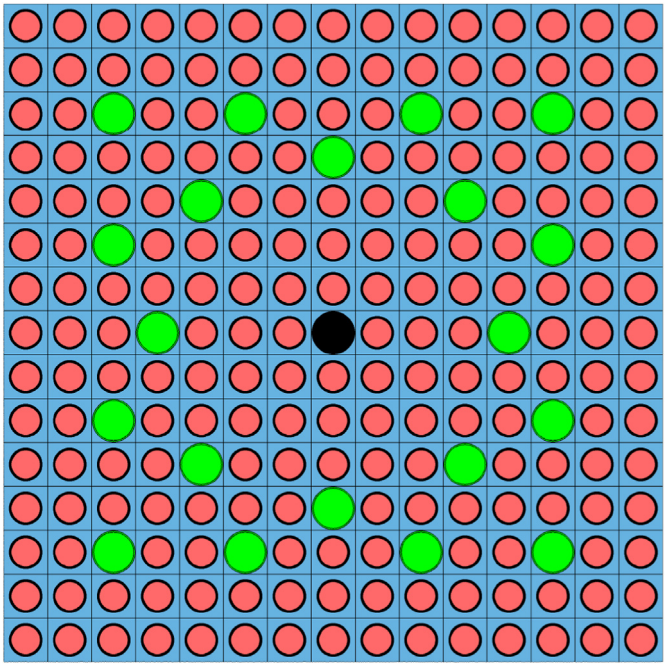

Fig. 3. Radial layout of assembly C01.
Legend: UO_2 (red), moderator (blue), guide tube (green), instrument tube (black). (For interpretation of the references to color in this figure legend, the reader is referred to the Web version of this article.)

Table 1
Modeling parameters and their uncertainties.

Parameter	Nominal value	Uncertainty (%)	Distribution
Fuel density	10.227 g/cc	0.41	Uniform
^{235}U enrichment	3.095 wt%^{235}U	0.54	
Pellet radius	0.4645 cm	0.54	
Clad outer radius	0.5360 cm	1.55	
Fuel temperature	900 K	3.33	
Power density, cycle 1	10.93 W/g	1.67	
Power density, cycle 2	35.22 W/g		
Power density, cycle 3	24.26 W/g		
Power density, cycle 4	29.20 W/g		
Mod Temp	577 K	2.00	
Boron Conc.	650 ppm	2.00	

Table 2
Other modeling parameters of assembly C01.

Assembly pitch	21.50 cm
Rod pitch	1.43 cm
Clad thickness	0.0618 cm
Moderator density	0.72 g/cc
Guide tube outer radius	0.6935 cm
Guide tube inner radius	0.6505 cm
Operating days (4 cycles)	1029/267/312/290
Downtime days	85/56/442

3. Computational models and methods

3.1. STREAM

STREAM is a reactor analysis code for multigroup cross section generation, criticality, and depletion calculations. STREAM neutron transport solution is based on the method of characteristics (MOC) and the resonance treatment employs the pin-based slowing down method (PSM) [27] or the equivalence theory's two-term rational approximation [28,29]. STREAM features a source term calculation module and can calculate pin-wise or assembly wise spent fuel nuclide concentrations, radio activity, decay heat, neutron, and gamma radiation spectra, for applications in burnup credit criticality safety and deep penetration shielding analysis. STREAM can also stochastically sample the nuclear reaction cross section covariance from evaluated nuclear data file ENDF/B-VII.1 to produce perturbed multigroup cross section for its calculations. The following multigroup cross section covariances are considered: covariance between scattering cross sections, covariance between scattering and fission cross sections, covariance between scattering and capture cross sections, covariance between fission cross sections, covariance between fission and capture cross sections, covariance between capture cross sections, covariance between number of neutrons generated per fission, and covariance between fission spectra. Covariances do not exist for all nuclides in the ENDF/B-VII.1 library. Only those nuclides which have covariances are considered. The covariance matrix employs zero matrix for nuclides without covariance in the ENDF library. The stochastic sampling of nuclear data in STREAM is described in detail in reference [30]. In the current study, only the nuclear reaction cross section covariance and perturbed fission product yields are considered among

the nuclear data. The perturbed fission product yields used in STREAM are directly generated by the authors using the SANDY code [31]. SANDY applies the generalized least-square method and conservation laws to the fission product yield and uncertainty data in nuclear data library to produce covariance of fission product yield. Then the fission product yields are updated, and perturbed information is obtained by sampling from a multivariate normal distribution [32]. Perturbed fission product yield for the fission of 31 materials and 3 neutron energies (thermal, 0.5 MeV and 14 MeV) are considered. The decay data (half-lives, branching fractions) are not perturbed. Moreover, the covariance between different nuclides, and the correlations between nuclear data and modelling parameters are not considered. In addition to the microscopic cross section, the resonance integral produced by the NJOY code are perturbed by STREAM to take the self-shielding effect of resonance into account while the self-shielding effect is not considered in the covariance matrix.

3.2. MCS

The Monte Carlo code MCS is used in this work to transport the neutron and photons in criticality and shielding calculations. MCS is a three-dimensional (3D) continuous energy neutron-transport Monte Carlo code under development at UNIST. MCS solves criticality, depletion, thermal hydraulics, fixed-source and shielding problems. The code has been validated against ~300 critical cases of the International Criticality Safety Benchmark Experimental Problem (ICSBEP), VERA benchmark, and BEAVRS benchmark [33,34]. The photon fixed-source runs of MCS have been verified against reference Monte Carlo codes for shielding problems [35]. The nuclear data employed in MCS calculations in this work are not perturbed. These include the ENDF/B-VII.1 continuous energy neutron cross section data for neutron transport, the eprdata12 library for photon transport [36] and the flux-to-dose conversion coefficients [37,38]. In this paper, the kind of dose focused on is the effective dose and isotropic irradiation condition is considered. However, flux-to-dose conversion coefficients for other irradiation conditions (antero-posterior, postero-anterior, left lateral, right lateral, rotational) can be used in MCS.

3.3. Calculation conditions

STREAM depletes the fuel assembly shown in Fig. 3 using one-eighth symmetry and the information listed in Table 1–2, to calculate the source terms with pin level resolution. The perturbed model parameters are generated using Latin Hypercube Sampling (LHS). The input parameters in Table 1 are assumed to be independent. ENDF/B-VII.1 cross section data is employed in the STREAM calculations with a two-dimensional (2D) model of the assembly and a reflective boundary condition. STREAM simulations assessed the individual effects of three groups: uncertainties in (1) cross section (2) fission product yields and (3) assembly modeling parameters. For each of the three groups, 300 perturbed calculations were performed. All parameters presented in Table 1 are perturbed simultaneously for the modeling parameters group. The 72 group cross section used by STREAM calculation, resonance integral and fission product yields are perturbed among the nuclear data. For each of these perturbations, the neutron and gamma spectra are calculated. In total, 900 STREAM simulations were performed. The source terms at a cooling time of 23 years are used in the MC shielding calculations.

The perturbed assembly model parameters used in STREAM such as pellet radius, clad outer radius and fuel temperature are carried over into the TN-32 cask MCS model in their perturbed state. The model specifications of the TN-32 cask are however not perturbed in this analysis. These might have their contributions since they will be considered in the particle transport during the criticality and shielding calculations. Correlations between nuclide concentrations calculated by STREAM are not considered explicitly in propagating the nuclide concentration uncertainties in MCS calculations. The correlations between nuclide concentrations are only implicitly treated in STREAM. The perturbed nuclide concentrations from STREAM are used directly in MCS transport simulations as is. This might affect the cask effective multiplication factor and dose rate. One study reports the effect of considering correlations between nuclide concentrations on the cask effective multiplication factor as 100 pcm [8]. In addition, the correlations between the source spectra in different energy groups are not considered. All the MCS criticality simulations are performed with the cask filled with water. The shielding simulations are performed with cask filled with air and MCS runs in fixed-source mode. All 32 spent fuel assemblies loaded into the cask are identical. The compositions are the same in all the assemblies. However, the pin-wise composition and radiation spectra in each assembly are modeled differently and axial variations are not considered. The spacer grids of the assembly is not modeled, and we homogenized the top and bottom nozzles. The photon calculations use the thick-target bremsstrahlung option, turns on the bremsstrahlung treatment for positrons, activates the atomic relaxation and the Doppler broadening for Compton-scattered photons. Determination of the radiation dose level outside of the TN-32 cask is a complex deep penetration shielding problem because of the 36.855 cm thick radial shield. The 10 statistical tests in MCS are used in this work to assess tally convergence [39]. Only the uncertainties of the cask surface dose rates are analyzed. Considerations for the dose rates uncertainties at some meters away from the cask is left for future work. The internal weight window (WW) variance reduction technique (VRT) in the MCS code was used in the neutron shielding calculations [40]. This ensures that we do not run large number of histories and we are able to obtain relative statistical error less than 10%. The neutron dose calculation uses a cylindrical mesh ($r\theta z = (30, 4, 64)$ grid) to cover the TN-32 geometry for the WW generation. For the neutron dose calculation outside the cask, the dose is tallied in a 10 cm $\times$ 10 cm $\times$ 10 cm box placed on the cask surface at the axial mid-plane. A total of 5 million neutrons are simulated in each fixed-source neutron shielding simulation. For each input with perturbed data, a maximum of four WW iterations are required during the neutron shielding for the neutron dose tally to pass all the 10 statistical checks. The neutron-photon coupled simulation to determine the secondary photon dose rate employs a total of 20 million neutrons and realizes a relative statistical error less than 10%, with no VRT applied. For the primary photon dose shielding calculations on the cask surface, both MCS and MCNP could not produce at least one non-zero score in the tally region outside the cask for the WW generator, due to the difficulty for the photons to penetrate the cask shielding materials. Moreover, the point detector tally of MCS is under development. Thus, the point detector (F5) tally of MCNP was employed. Besides, after many iterations, the WW generated by MCNP still has a lot of zero importance meshes where no scoring particle has reached, and this WW could not reduce the F5 tally error to less than 5%. It was thus decided to generate the importance for biasing the MC simulation by a deterministic code that calculates the adjoint flux. The point detector location is at a point 5 cm from the cask surface (corresponding to the center of the tally box in the neutron case). A number of history to yield primary photon dose relative statistical error less than 5% was used for the point detector calculations. The primary photon calculation simulates 800 million photons, combined with WW generated from the deterministic code DENOVO in the MAVRIC code system [18]. The importance map from the

deterministic code is converted into WW lower bounds in the format which can be used in MCNP. The deterministic importance map used in the photon shielding VR is generated in a cartesian mesh that overlays the geometry discretized into a 30 × 30 × 63 spatial grid and 19-energy groups. In this work, please note that the biased source from MAVRIC was not used in MCNP, and only one MCNP calculation was run for each perturbed input *i.e.*, no successive WW iteration was performed when the importance map comes from the deterministic code. The MC simulations considered the separate impacts of nuclear data and modeling parameter uncertainties on the calculated dose rates using calculations which employ perturbed nuclide concentrations and radiation spectra. A total of 900 MC simulation was performed. For each MC criticality calculation, 50 inactive, 500 active and 30,000 neutrons are simulated. Please note that the efficiency of the VRTs is not the subject of discussion in this paper, hence, the figures of merits are not presented or commented upon.

4. Results and discussions

MCS model of the TN-32 cask has been verified against MCNP in criticality and shielding calculations. The verification results can be found in the previous works. Hence, no further verification is conducted in this paper and the discussion is focused on analyzing the nuclear data and model parameter induced uncertainties of the MCS results. The neutron and photon source spectra are calculated by STREAM in 16 and 39 energy groups, respectively. The neutron sources consist of neutrons from (α,n) reactions and spontaneous fission. Actinides in spent fuel decay by emitting alphas which interact with oxygen present in oxide fuel. The photon sources are composed of X-rays, decay gamma, spontaneous fission gamma, (α, n) reaction gamma and bremsstrahlung from β^- and β^+ particles slowing down in oxide fuel material. Assembly wise neutron and photon spectra calculated with unperturbed nuclear data and nominal model parameters are illustrated in Fig. 4. Most of the neutrons come from spontaneous fission. The largest neutron intensities are concentrated in the 0.1–5 MeV energy range. The dominant neutron source is ^{244}Cm which makes up 94% of the total neutron source at 23 years cooling. About half of the photon sources are emitted in the low energy range at less than 100 keV. A sharp peak is observed on the photon spectra plot in the 0.65–0.7 MeV energy range. This corresponds to the 661.7 keV peak of ^{137}Cs.

4.1. Uncertainty propagation during depletion and source term calculation

The uncertainties of assembly wise neutron and photon source calculated with perturbed nuclear data and perturbed model parameters are presented in Fig. 5 as a function of the energy groups. The neutron source uncertainty remains almost constant across the energy groups with an uncertainty of 9% from the cross section data dominating and 6.5% from the design parameters/operating conditions. Except otherwise stated, the uncertainties presented are relative, calculated as the ratio of standard deviation to mean of perturbed outputs. Below 2 MeV, the photon source uncertainties due to cross section are small while the fission yields dominate the photon source uncertainties. The photon source uncertainties become larger (around 6–9%) between 2.2 and 11 MeV as the photon source decrease in intensity. The photon source uncertainties in fast energy region due to uncertainties of cross section and modeling parameters seems to be dominant. However, the absolute uncertainties in that region is very small because the photon spectra in that region is negligible as shown in Fig. 4. The total absolute uncertainties can be seen in Section 4.3. Fig. 5 shows that the neutron and photon source uncertainties coming from the design parameters operating conditions are not negligible and should be considered.

The uncertainty analysis results are from 300 samples of each input data. Larger number of samples could not be employed due to the computational cost. Nevertheless, it is important that the quantities analyzed are converged. Fig. 6 shows the convergence of uncertainties of the neutron and photon sources as a function of number of samples for the perturbed nuclear data and modeling parameters. This figure also indicates that around 150 perturbed samples might be enough to obtain fairly converged uncertainties for the case analyzed. This is important especially for the MC shielding calculations that are computationally expensive if we want to obtain reasonable statistical error.

The uncertainties of neutron and photon sources across the fuel pins are shown in Fig. 7. The white color region in this figure are the assembly guide tubes. Fig. 7 shows that the neutron source uncertainties are least driven by the fission yields and dominated by the cross section, design, and operation data uncertainties. On the other hand, the photon source uncertainties are mostly driven by the fission yields, design, and operation data uncertainties, while the cross section data have insignificant contributions. For the

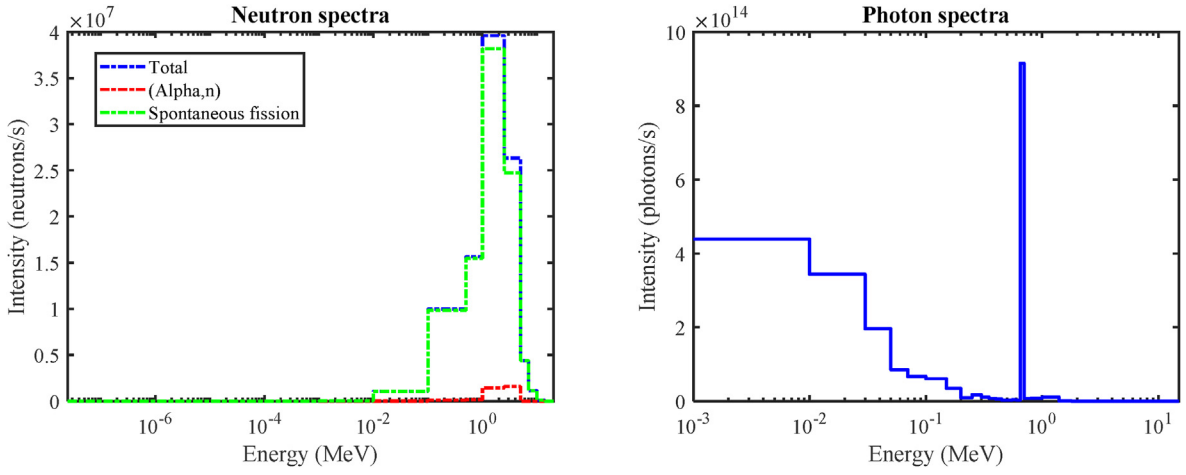

Fig. 4. Assembly neutron and photon spectra of nominal case at 23 years of cooling.

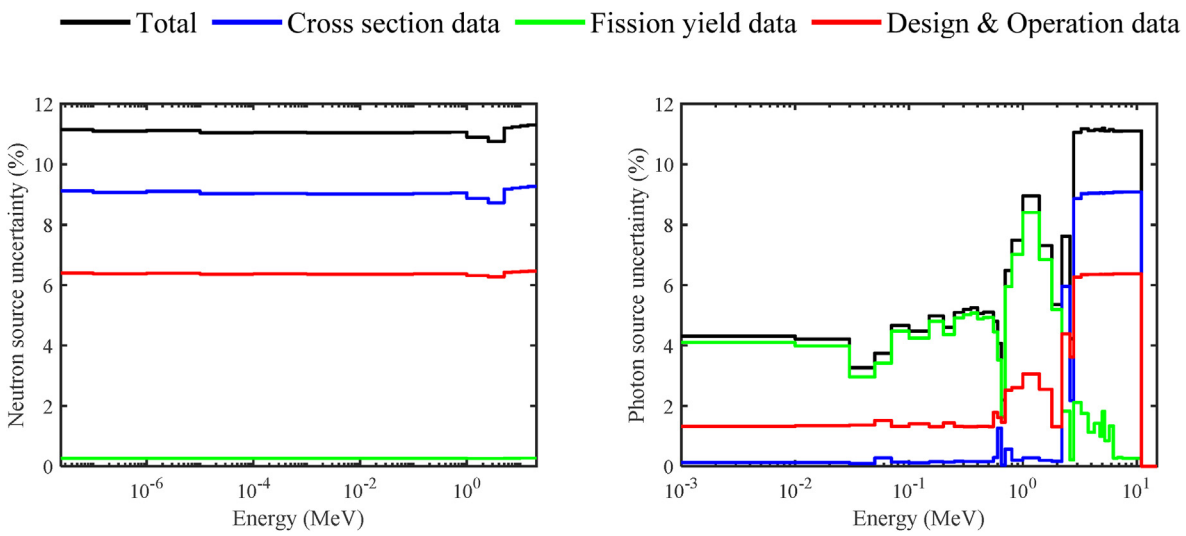

Fig. 5. Uncertainties of assembly neutron and photon spectra at 23 years of cooling.

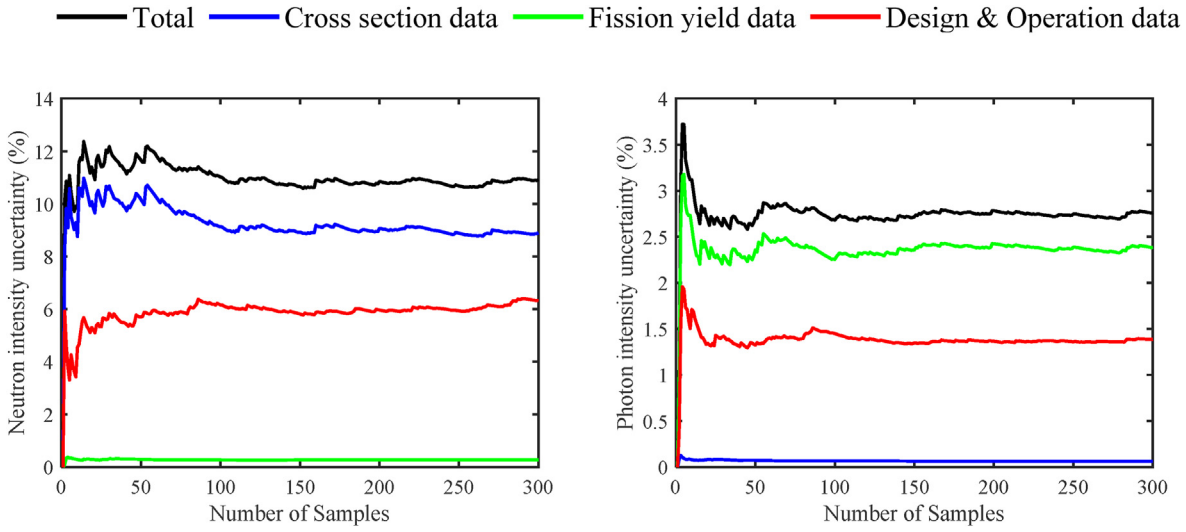

Fig. 6. Convergence of assembly neutron and photon source uncertainty.

neutron source uncertainty, the aforementioned observation stays the same for up to 10,000 years as can be seen in Fig. 8. However, the photon source uncertainty becomes less dependent on the fission yields beyond 100 years, when the cross section, design, and operation data uncertainty dominate. This is illustrated in Fig. 8.

4.2. Uncertainty propagation during shielding calculation

The neutron and photon dose rates are computed by the convolution of the MC neutron and photon flux per particle source, respectively, with the isotropic flux-to-dose conversion coefficients using log-log interpolation, then multiplying by the total neutron and photon source strength of the 32 assemblies. Fig. 9 shows the convergence of uncertainties of the neutron dose rate on the cask surface, as a function of number of samples for the perturbed nuclear data and modeling parameters. It can be seen from this figure that around 150 perturbed samples are sufficient to obtain converged neutron dose rate uncertainties. A similar observation is found in Fig. 6 for the convergence of input uncertainties. This implies that we might not need to run up to 300 cases of MC shielding calculations to obtain the neutron dose rate uncertainties caused by each of the three groups of uncertain input data (cross section, fission yields, design parameters and operating conditions) considered. The uncertainties of the neutron and photon source intensities and neutron and photon dose due to the various perturbed input data are compared in Table 3 – 6 as a function of number of samples (*N* samples). For the neutron case, the results produced by 100 samples shows some slight variation compared to those of the 150 and 300 samples. Although this difference is due to the convergence of stochastic quantities, it is observed that the uncertainties at these number of samples are not changed much.

The results of uncertainties are presented in Table 7, and these correspond to those of 300 perturbed samples from each set of input data. These cask neutron dose results display similar trend to the assembly neutron source uncertainties in Fig. 5. The fission yields have the smallest contribution to the neutron dose uncertainties, followed by the design parameters and operating conditions (*i.e.*, the modeling parameters in Table 1) having the second largest contribution, and the cross-section data with the largest contribution. Majority of the neutron source is dominated by the

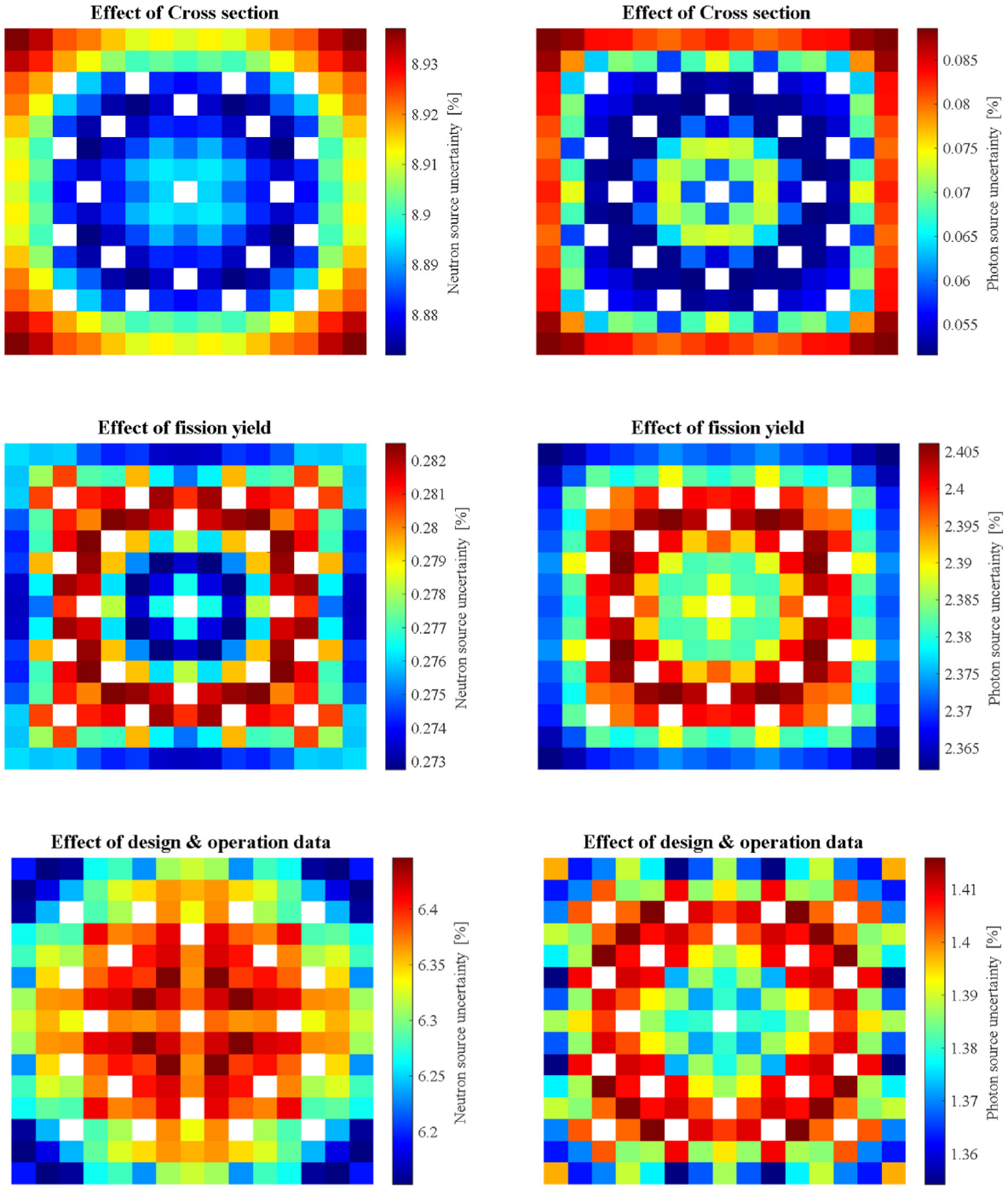

Fig. 7. Uncertainties of pin neutron source (left) and photon source (right) at 23 years.

actinides. Please note that the TN32 SNF assembly cask analyzed in this work is loaded with the same 15 × 15 assembly, with same source terms and isotopic number densities, but varying number densities, neutron, and gamma source spectra from pin to pin in the assembly. This could be the reason why the assembly neutron source uncertainties and cask neutron dose uncertainties have similar trends in contributions from the cross section data, fission yields and modeling parameters. It seem reasonable to infer that for cases in which different assemblies with different intensities of neutron source terms are loaded into the cask, the neutron dose will likely be influenced by the assembly with most dominant neutron radiation source in terms of intensity and/or energy. This is confirmed from the fact that more source particles will be sampled from those assemblies and source energy groups with the highest intensities since this defines the source sampling probability and cumulative density functions. The neutron dose rate uncertainties are only calculated with the cask loaded with SNF assemblies cooled up to 23 years. However, based on Fig. 8, we can predict what will be the major contributors to the uncertainties at longer cooling times. Comparing Figs. 6 and 9, it could be seen that although the fission yield contribution to the neutron source uncertainty is low at about 0.3%, the contribution to the neutron dose

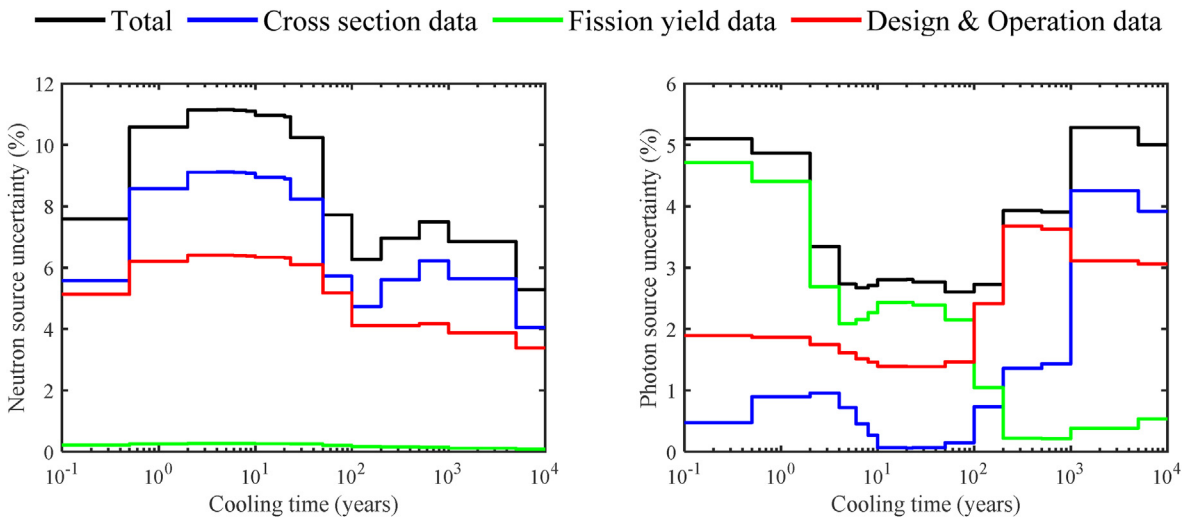

Fig. 8. Uncertainties of assembly neutron and photon intensity versus cooling time.

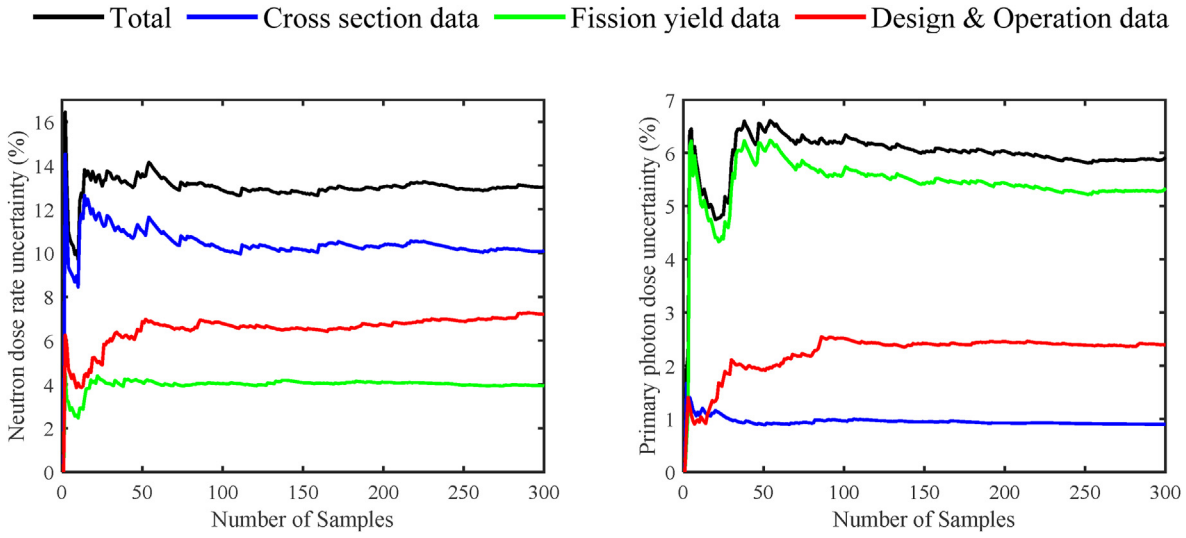

Fig. 9. Convergence of cask neutron and photon dose rate uncertainty.

Table 3
Neutron source uncertainty (%).

N samples	Cross section	Fission yields	Modeling parameters	Total
100	9.14	0.27	6.16	11.02
150	8.93	0.27	5.81	10.66
300	8.90	0.28	6.32	10.92

Table 4
Neutron dose uncertainty (%).

N samples	Cross section	Fission yields	Modeling parameters	Total
100	10.17	4.05	6.78	12.88
150	10.14	4.09	6.53	12.73
300	10.11	3.94	7.21	13.03

Table 5
Photon source uncertainty (%).

N samples	Cross section	Fission yields	Modeling parameters	Total
100	0.07	2.25	1.45	2.68
150	0.06	2.36	1.35	2.72
300	0.06	2.39	1.39	2.76

Table 6
Photon dose uncertainty (%).

N samples	Cross section	Fission yields	Modeling parameters	Total
100	0.96	5.66	2.52	6.27
150	0.95	5.42	2.41	6.00
300	0.90	5.34	2.39	5.92

uncertainty is about 4% after the propagation. Comparing Fig. 8 and Table 7, we observe that the total uncertainty of the neutron source at 23 years cooling is about 11%, while the neutron dose rate at the cask surface has a total of about 13% uncertainty from all the perturbed data. Also note, the total uncertainty of the major neutron source ^{244}Cm in our previous UQ work [5] is not much different from (*i.e.*, appears to be consistent with or comparable to) the total neutron dose uncertainty.

Table 7
Uncertainty results.

	Perturbed data			
	Cross section	Fission yields	Modeling parameters	Total
Neutron dose, μSv/h	14.51	14.78	15.05	
Uncertainty, %	10.11	3.94	7.21	13.03
Maximum statistical error, %	6.44	5.59	5.13	
Primary photon dose, μSv/h	2.90E+03	2.83E+03	2.95E+03	
Uncertainty, %	0.90	5.34	2.39	5.92
Maximum statistical error, %	4.21	3.60	4.66	
Secondary photon dose, μSv/h	3.21	3.29	3.10	
Uncertainty, %	9.58	4.82	9.58	14.38
Maximum statistical error, %	7.68	8.54	8.61	
Average *k-eff*	0.7084	0.7086	0.7088	
Uncertainty, pcm	518	344	1049	
Maximum statistical error, pcm	15.83	15.58	15.43	

The primary photon dose on the cask surface is large, on the order of $>2 \times 10^3$ μSv/h. Moreover, the total neutron plus photon dose on the cask surface exceeds the regulatory limit of 2,000 μSv/h. This is an example of a case in which the total dose needs to be checked whether it is within the permissible limit. Although, the unperturbed effective multiplication factor is shown in Table 7 as 0.7079 ± 14 pcm and this satisfies the criticality safety requirement $k_{eff} < 0.95$. The fact that the multiplication factor is far below 0.95 justifies ignoring correlations between nuclide concentrations mentioned in section 3.3. In reality, the same type of assembly with parameters (enrichment, burnup and cooling time) considered in this work might not be loaded into the TN32 cask for radiation safety purposes. The loading pattern should be optimized to satisfy safety requirements, although this is beyond the scope of this work. Despite the fact that the total dose did not satisfy the radiation safety requirement, and this could have had an effect on the total uncertainty, the loading pattern is however used in this work to demonstrate the shielding UQ. The purpose of the analysis is to identify the major contributors to the dose uncertainties. The cross section contribution to the photon source uncertainty is small (0.06%, see Fig. 6), while the contribution to the photon dose is around 1% as shown in Fig. 9. Fig. 9 and Table 7 confirms what we observed in Fig. 6. The fission yield is the largest contributor to the primary photon dose uncertainty at 5.3%, followed by the modeling parameters at 2.4%. The least contribution is from the cross section data (0.9%). Most of the photon source come from the fission products. The fission yield contribution to the photon source uncertainty is 2.4% while the contribution to the primary photon dose uncertainty is more than twice at 5.3% after the propagation. The fission yield uncertainties appears to be the reason why the photon source and dose uncertainties are not comparable, as in the neutron case. At 23 years, the photon source has total uncertainty of about 2.8% (see Fig. 8), while as shown in Table 7, the primary photon dose rate has total uncertainty of roughly 6% due to the nuclear data and modeling parameter uncertainties. Because of the large photon dose rate, the uncertainty is smaller (at 6%) than that of the neutron dose (13%). The total uncertainties in the tables and figures quadratically sums the three different sources of uncertainties (cross section, fission yield, and modeling parameters), assuming they are not correlated.

In Table 7, the secondary photon dose is small (~3μSv/h) considering that the cooling time of 23 years is long, and this is long enough time for activation products (if produced) in the structural components (clad, end springs, plugs, plenum, bottom and top nozzle) to have decayed. Another reason for the small secondary photon dose could be because of the small contents of nuclides (if at all present) whose irradiation leads to activation products in the structural components. The secondary photon dose is much smaller than the neutron dose. The cross section and modeling parameters have similar contributions of 9.6% to the secondary photon dose uncertainties while fission yield induced uncertainty is ~5%.

Without performing the uncertainty propagation in the shielding calculation, it seem possible to predict the total neutron dose uncertainties from the total neutron source uncertainties. Although this is not the case for the total photon dose and source uncertainties. This is important considering the computational requirements of deep penetration shielding calculations, even when VRT are employed. Most importantly, based on the results shown in Tables 3–7, it can be inferred that it is unnecessary to perturb the fission yield to determine the total uncertainty of the neutron dose. Similarly, to determine the photon dose uncertainty, the cross section data need not be perturbed.

4.3. Statistical errors and confidence intervals of the uncertainty estimates

The uncertainty quantification in this study is conducted by random sampling. Because of the probabilistic nature of the use of random numbers and the finite number of sampling, the uncertainty estimates in themselves have statistical error which should be quantified in the form of confidence intervals to judge the reliability and accuracy of the uncertainty estimates and for the purposes of convergence analysis. Depending on the probability distribution of the quantities of interest (radiation source and dose rate), the statistical error of their uncertainties can be estimated from chi-squared distribution if the quantities of interest follow a Gaussian distribution, in which case the assumption of normality holds [41]. Another method should be considered such as the bootstrap method if the quantities of interest do not follow a Gaussian distribution.

Although the statistical error estimation for the uncertainties in this paper will be dealt with comprehensively and in detail in future work, we summarize an estimate of the statistical error of the uncertainty analysis results. Please note in this case it is assumed that the radiation source and dose rate follow a normal distribution. For Figs. 6 and 9, the confidence interval computed for the standard deviation (*i.e.*, absolute uncertainties) are shown in Figs. 10 and 11. The photon and neutron sources are of the order of 10^{15} and 10^8, respectively, as shown in Fig. 4. Only the confidence intervals of the total absolute uncertainties are presented. The total absolute uncertainties is the quadratic sum of all uncertainties coming from the perturbed cross section, fission yield, and modeling parameters

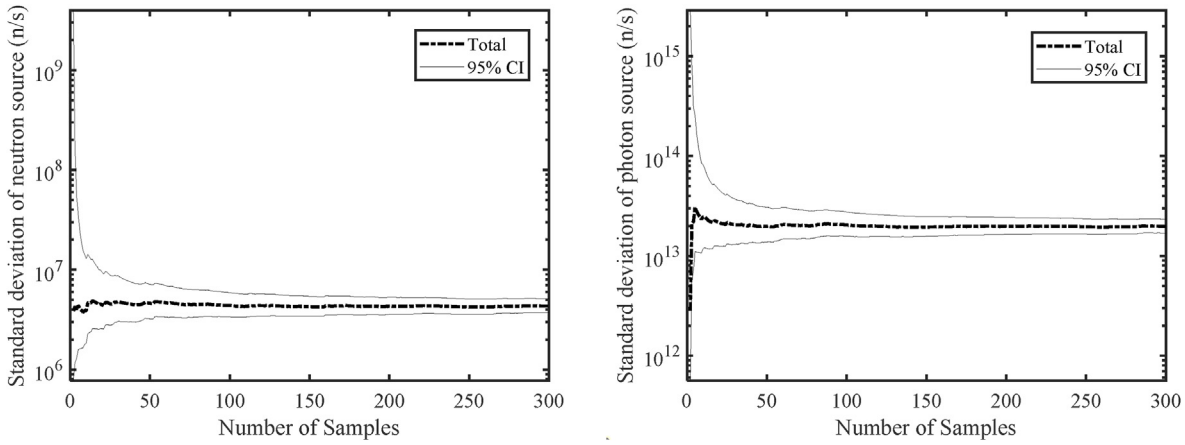

Fig. 10. Convergence of neutron and photon source standard deviation. The black band is the 95% confidence interval of the standard deviation.

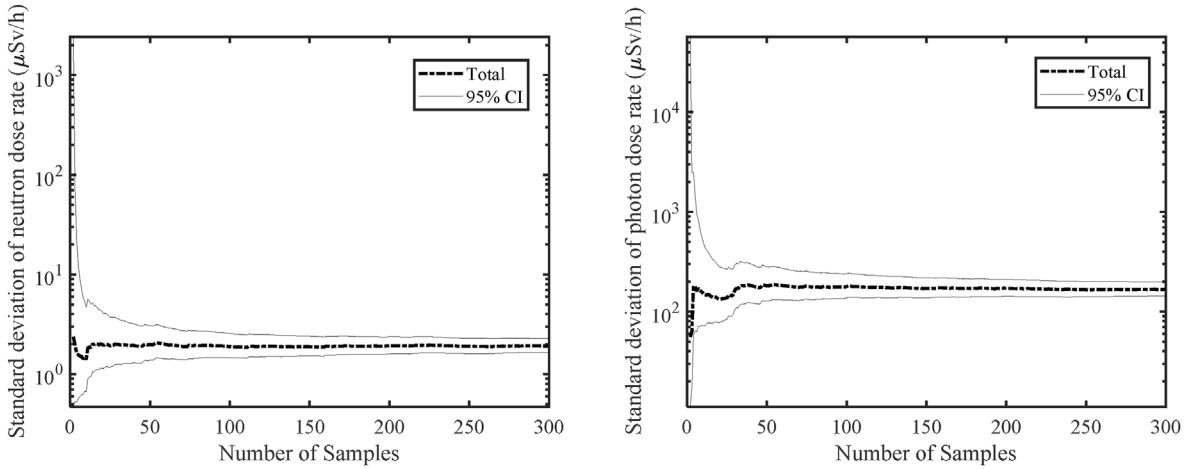

Fig. 11. Convergence of neutron and photon dose standard deviation. The black band is the 95% confidence interval of the standard deviation.

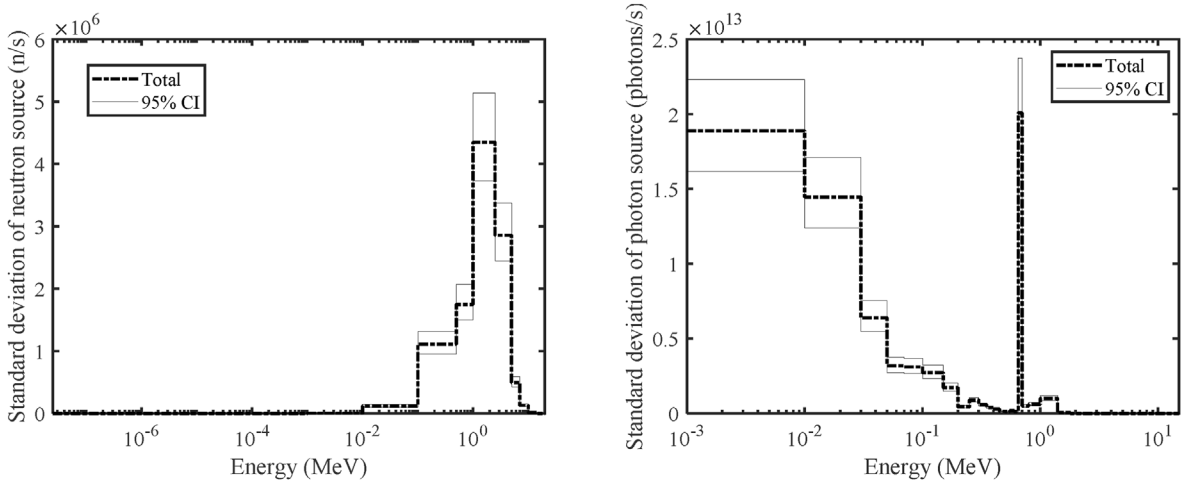

Fig. 12. Absolute uncertainty of neutron and photon spectra showing the 95% confidence intervals.

(design and operating conditions). For Figs. 5 and 8, the confidence interval computed for the standard deviation (*i.e.*, absolute uncertainties) are shown in Figs. 12 and 13. The absolute uncertainty of the radiation source spectra follows the same trend as the actual radiation spectra. The absolute uncertainty of the radiation source during cooling decreases just as the radiation source decreases during the cooling time. The confidence intervals in Figs. 10–13 are computed according to equations (13) and (14) in Ref. [42].

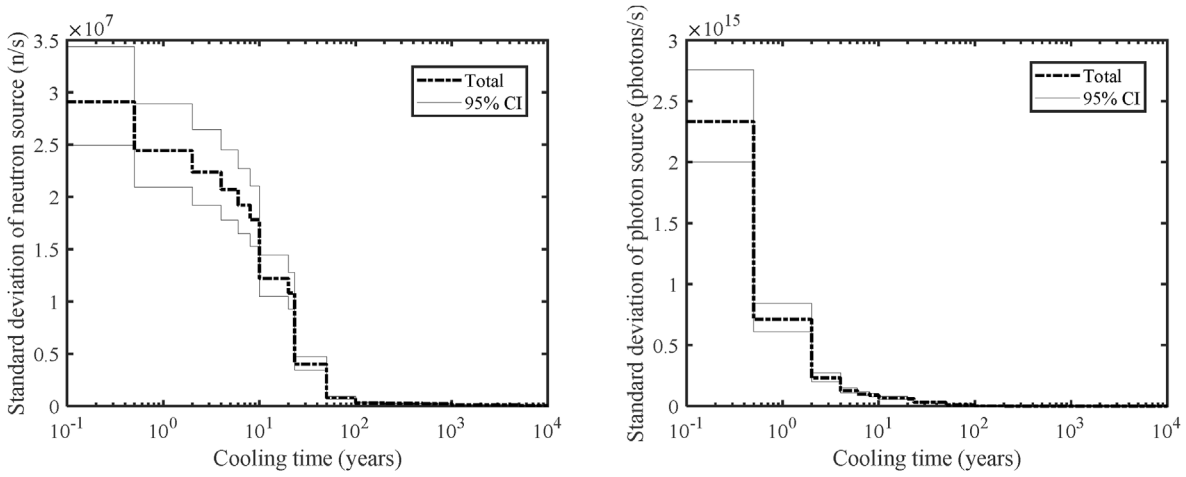

Fig. 13. Absolute uncertainty of neutron and photon intensity showing the 95% confidence intervals.

5. Conclusions

Radiation source uncertainties are propagated to SNF cask shielding calculations. The uncertainty propagation applies the nuclide inventories and radiation source outputs of the STREAM code as inputs of the transport calculations of the MC codes MCS and MCNP6. The dose rate uncertainties are quantified due to nuclear data and modeling parameters. The nuclear data uncertainties are obtained from the stochastic sampling of the cross-section covariance and perturbed fission product yields. The modelling parameters uncertainties are based on perturbed design parameters and operating conditions. Uncertainties coming from these sources are first propagated to the nuclide inventories and radiation source terms, and then secondly propagated to the dose rate on the cask surface. For the neutron dose and secondary photon dose, the uncertainties are dominantly affected by the cross section data and assembly modeling parameters, with the fission yield data impacting the uncertainties in a relatively small way. For the neutron dose and secondary photon dose on the cask surface, the uncertainties can be up to 13% and 14%, respectively. The primary photon dose on the cask surface is shown to have an uncertainty of about 6% and this is mostly influenced by the fission yield data and modeling parameters, as the cross section data have a comparatively small effect. For the neutron and secondary photon dose, the uncertainties (13% and 14%, respectively) are low. The neutron and secondary photon dose in themselves are low at ~15 μSv/h and ~3 μSv/h, respectively. However, the primary photon dose is high (~2.9 × 10^3 μSv/h) and this makes the total dose to exceed the limiting value (2.0 × 10^3 μSv/h). Thus, the photon dose uncertainty on the cask surface (~6%) is high and this uncertainty (174 μSv/h) exceeds what is supposed to be the limit of neutron dose at 2 m away from the cask surface (100 μSv/h). The cask shielding UQ results are significant because they are reported for the first time in this work. The major contributors to the uncertainty of predictions are identified highlighting which of the input data (cross sections, fission yields and modeling parameters) to work on. The assembly design parameters and operating conditions which are often neglected in the available SNF UQ literature are shown in this work to be non-negligible and an important source of uncertainties. Although the reported uncertainties pertain to a cask loaded with the same assemblies, it gives the order of magnitude for the uncertainties in an SNF cask shielding calculation. Besides, this may be different for other cases for which the loaded assemblies have different enrichments, burnups and cooling times. This will be analyzed as part of future works.

In the next phase of this work, further verification or validation of the UQ results will be conducted. Other uncertainties such as Cobalt content of the hardware region, axial burnup profile, cask geometry, and material densities will be considered. The effect of uncertainties from assemblies in the periphery versus center locations, on the dose rate, will be examined. An SNF cask with optimized loading pattern of assemblies with different enrichments, burnups and cooling times will be analyzed in future UQ process.

Declaration of competing interest

The authors declare that they have no known competing financial interests or personal relationships that could have appeared to influence the work reported in this paper.

Acknowledgments

This work was supported by the National Research Foundation of Korea (NRF) grant funded by the Korea government (MSIT). (No. NRF-2019M2D2A1A03058371).

References

[1] J. Choe, et al., Verification and validation of STREAM/RAST-K for PWR analysis, Nucl. Eng. Technol. 51 (2) (2019) 356, https://doi.org/10.1016/j.net.2018.10.004.
[2] N.N.T. Mai, et al., Extension of Monte Carlo code MCS to spent fuel cask shielding analysis, Int. J. Energy Res. 44 (10) (2020) 8089, https://doi.org/10.1002/er.5023.
[3] B. Ebiwonjumi, et al., Validation of lattice physics code STREAM for predicting pressurized water reactor spent nuclear fuel isotopic inventory, Ann. Nucl. Energy 120 (2018) 431, https://doi.org/10.1016/j.anucene.2018.06.002.
[4] B. Ebiwonjumi, et al., Verification and validation of radiation source term capabilities in STREAM, Ann. Nucl. Energy 124 (2019) 80, https://doi.org/10.1016/j.anucene.2018.09.034.
[5] B. Ebiwonjumi, et al., Uncertainty quantification of PWR spent fuel due to nuclear data and modeling parameters, Nucl. Eng. Technol. 53 (3) (2021) 715, https://doi.org/10.1016/j.net.2020.07.012.
[6] H. Yun, et al., ' "an efficient evaluation of depletion uncertainty for a GBC-32 dry storage cask with PLUS7 fuel assemblies using the Monte Carlo uncertainty sampling method, Ann. Nucl. Energy 110 (2017) 679, https://doi.org/10.1016/j.anucene.2017.07.020.
[7] I.C. Gauld, U. Mertyurek, Validation of BWR spent nuclear fuel isotopic predictions with applications to burnup credit, Nucl. Eng. Des. 345 (2019) 110, https://doi.org/10.1016/j.nucengdes.2019.01.026.
[8] M.I. Radaideh, D. Price, T. Kozlowski, On using computational versus data-driven methods for uncertainty propagation of isotopic uncertainties, Nucl. Eng. Technol. 52 (6) (2020) 1148, https://doi.org/10.1016/j.net.2019.11.029.
[9] J. Jang, et al., Uncertainties of PWR spent nuclear fuel isotope inventory for back-end cycle analysis with STREAM/RAST-K, Ann. Nucl. Energy 158 (2021)

108267, https://doi.org/10.1016/j.anucene.2021.108267.
[10] B.T. Rearden, et al., TSUNAMI Primer: A Primer for Sensitivity/Uncertainty Calculations with SCALE," ORNL/TM-2009/027, Oak Ridge National Laboratory, 2009.
[11] M. Williams, et al., A statistical sampling method for uncertainty analysis with SCALE and XSUSA, Nucl. Tech. 183 (3) (2013) 515, https://doi.org/10.13182/NT12-112.
[12] I.C. Gauld, et al., Isotopic depletion and decay methods and analysis capabilities in SCALE, Nucl. Tech. 174 (2) (2011) 169, https://doi.org/10.13182/NT11-3.
[13] S. Goluoglu, et al., Monte Carlo criticality methods and analysis capabilities in SCALE, Nucl. Tech. 174 (2) (2011) 214, https://doi.org/10.13182/NT10-124.
[14] T. Goorley, et al., Initial MCNP6 release overview, Nucl. Tech. 180 (3) (2012) 298, https://doi.org/10.13182/NT11-135.
[15] H. Lee, et al., MCS – a Monte Carlo particle transport code for large-scale power reactor analysis, Ann. Nucl. Energy 139 (2020) 107276, https://doi.org/10.1016/j.anucene.2019.107276.
[16] A. Haghighat, J.C. Wagner, Monte Carlo variance reduction with deterministic importance functions, Prog. Nucl. Energy 42 (1) (2003) 25, https://doi.org/10.1016/S0149-1970(02)00002-1.
[17] J. Sweezy, et al., Automated variance reduction for MCNP using deterministic methods, Radiat. Protect. Dosim. 116 (2005) 508, https://doi.org/10.1093/rpd/nci257.
[18] D.E. Peplow, Monte Carlo shielding analysis capabilities with MAVRIC, Nucl. Tech. 174 (2) (2011) 289, https://doi.org/10.13182/NT174-289.
[19] J.H. Ko, et al., Shielding analysis of dual purpose casks for spent nuclear fuel under normal storage conditions, Nucl. Tech. 46 (4) (2014) 547, https://doi.org/10.5516/NET.08.2013.039.
[20] Y. Gao, et al., Radiation dose rate distributions of spent fuel dry casks estimated with MAVRIC based on detailed geometry and continuous-energy models, Ann. Nucl. Energy 117 (2018) 84, https://doi.org/10.1016/j.anucene.2018.03.015.
[21] Inc Transnuclear, TN-32 dry storage cask system safety evaluation report," United States nuclear regulatory commission. https://www.nrc.gov/docs/ML0036/ML003696918.pdf. (Accessed 1 September 2021).
[22] U.S.NRC, Packaging and transportation of radioactive material, 10 CFR 72," United States nuclear regulatory commission. https://www.nrc.gov/reading-rm/doc-collections/cfr/part072/. (Accessed 1 September 2021).
[23] U.S.NRC, TN-32 generic technical specification," United States nuclear regulatory commission. https://www.nrc.gov/docs/ML0104/ML010460423.pdf. (Accessed 1 September 2021).
[24] A.B. Svensk Kärnbränslehantering, Measurements of Decay Heat in Spent Nuclear Fuel at the Swedish Interim Storage Facility, CLAB," R-05-62, Swedish Nuclear Fuel and Waste Management Co, 2006.
[25] G. Ilas, H. Liljenfeldt, Decay heat uncertainty for BWR used fuel due to modeling and nuclear data uncertainties, Nucl. Eng. Des. 319 (2017) 176, https://doi.org/10.1016/j.nucengdes.2017.05.009.
[26] D. Rochman, et al., Best estimate plus uncertainty analysis for the 244Cm prediction in spent fuel characterization, in: Proc. ANS Best Estimate Plus Uncertainty International Conference (BEPU 2018), Real Collegio, Lucca, Italy, 2018, pp. 13–19. May.
[27] S. Choi, C. Lee, D. Lee, Resonance treatment using pin-based pointwise energy slowing-down method, J. Comput. Phys. 330 (2017) 134, https://doi.org/10.1016/j.jcp.2016.11.007.
[28] S. Choi, A. Khassenov, D. Lee, Resonance self-shielding method using resonance interference factor library for practical lattice physics computations of LWRs, J. Nucl. Sci. Technol. 53 (8) (2016) 1142, https://doi.org/10.1080/00223131.2015.1095686.
[29] S. Choi, et al., Resonance self-shielding methodology of new neutron transport code STREAM, J. Nucl. Sci. Technol. 52 (9) (2015) 1133, https://doi.org/10.1080/00223131.2014.993738.
[30] A. Yamamoto, et al., Uncertainty quantification of LWR core characteristics using random sampling method, Nucl. Sci. Eng. 181 (2) (2015) 160, https://doi.org/10.13182/NSE14-152.
[31] L. Fiorito, et al., Nuclear data uncertainty propagation to integral responses using SANDY, Ann. Nucl. Energy 101 (2017) 359, https://doi.org/10.1016/j.anucene.2016.11.026.
[32] L. Fiorito, et al., Generation of fission yield covariances to correct discrepancies in the nuclear data libraries, Ann. Nucl. Energy 88 (2016) 12, https://doi.org/10.1016/j.anucene.2015.10.027.
[33] J. Jang, et al., Validation of UNIST Monte Carlo code MCS for criticality safety analysis of PWR spent fuel pool and storage cask, Ann. Nucl. Energy 114 (2018) 495, https://doi.org/10.1016/j.anucene.2017.12.054.
[34] T. Nguyen, et al., Validation of UNIST Monte Carlo code MCS using VERA progression problems, Nucl. Eng. Technol. 52 (5) (2020) 878, https://doi.org/10.1016/j.net.2019.10.023.
[35] M. Lemaire, et al., Verification of photon transport capability of UNIST Monte Carlo code MCS, Comput. Phys. Commun. 231 (2018) 1, https://doi.org/10.1016/j.cpc.2018.05.008.
[36] H.H. Grady, An Electron/photon/relaxation Data Library for MCNP6," LA-UR-13-27377, Los Alamos National Laboratory, 2015.
[37] International Commission on Radiological Protection, Conversion coefficients for radiological protection quantities for external radiation exposures, Ann. ICRP, Publication 116 (2–5) (2010) 40, https://doi.org/10.1016/j.icrp.2011.10.001.
[38] International Commission on Radiological Protection, Corrigenda to ICRP publication 116: conversion coefficients for radiological protection quantities for external radiation exposures, Ann. ICRP, Publication 116 (2010) 40, https://doi.org/10.1177/0146645315577925, 2–5.
[39] M. Lemaire, H. Lee, D. Lee, Implementation of Tally Convergence Tests in UNIST Monte Carlo Code MCS, Transactions of the Korean Nuclear Society Autumn Meeting, Yeosu, Korea, 2018, pp. 24–26. October.
[40] P. Zhang, et al., Development of a Variance Reduction Scheme in the MCS Monte Carlo Code, Transactions of the Korean Nuclear Society Autumn Meeting, Yeosu, Korea, 2018, pp. 24–26. October.
[41] B. Foad, A. Yamamoto, T. Endo, Uncertainty and regression analysis of the MSLB accident in PWR based on unscented transformation and low rank approximation, Ann. Nucl. Energy 143 (2020) 107493, https://doi.org/10.1016/j.anucene.2020.107493.
[42] T. Endo, T. Watanabe, A. Yamamoto, Confidence interval estimation by bootstrap method for uncertainty quantification using random sampling method, J. Nucl. Sci. Tech. 52 (2015) 993, https://doi.org/10.1080/00223131.2015.1034216.